available at www.sciencedirect.com

ScienceDirect

journal homepage: www.elsevier.com/locate/chnjc

Article

Cu-doped mesoporous VO_x-TiO_2 in catalytic hydroxylation of benzene to phenol

XU Dan [a], JIA Lihua [a,*], GUO Xiangfeng [b,#]

[a] *College of Chemistry and Chemical Engineering, Qiqihar University, Qiqihar 161006, Heilongjiang, China*
[b] *Key Laboratory of Fine Chemicals, College of Heilongjiang Province, Qiqihar 161006, Heilongjiang, China*

ARTICLE INFO

Article history:
Received 27 September 2012
Accepted 7 November 2012
Published 20 February 2013

Keywords:
Copper
Vanadium species
Mesoporous titania
Benzene
Hydroxylation
Phenol

ABSTRACT

Liquid phase hydroxylation of benzene to phenol with hydrogen peroxide over VO_x-TiO_2 catalyst samples with Cu as a second metal was investigated. A series of Cu/VO_x-TiO_2 (vanadium loading was 4.3%) catalysts were prepared within the range of Cu loading (0.29%–2.5%) and calcined at the temperatures of 350–650 °C. The catalyst samples were characterized by N_2 adsorption-desorption, scanning electron microscopy, H_2 temperature-programmed reduction, X-ray diffraction, transmission electron microscopy, and X-ray photoelectron spectroscopy. After the addition of Cu, the Cu/VO_x-TiO_2 catalyst had more ordered mesoporous structure as compared with the VO_x-TiO_2 catalyst, and the vanadium was monodispersed on the TiO_2 support. The presence of Cu^{2+} ions on the catalyst surface was shown by XPS measurements. These Cu^{2+} ions probably contributed to the dispersion of vanadium on the surface of the TiO_2 support, and the more facile reduction of VO_x. The Cu^{2+} ions also strengthened the thermostability of the Cu/VO_x-TiO_2 catalyst. The effects of some other variables (Cu loading, catalyst amount, and reaction temperature) on the catalytic performance were also investigated.

1. Introduction

Phenol plays an important role in the chemical industry. More than 90% of the phenol is produced by the cumene process, which is a three step process that generates an equimolar amount of acetone as byproduct, and some waste products. Phenol synthesis by the direct hydroxylation of benzene is therefore attractive both economically and energetically [1]. Systems for the direct hydroxylation of benzene include the use of N_2O [2] or O_2 [3–6] in the vapor phase and H_2O_2 [7–9] in the liquid phase. The hydroxylation of benzene to phenol using H_2O_2 is probably the most effective route since it has high conversions and yields [10,11]. For the reaction with H_2O_2 as the oxidant, various solid catalysts under mild conditions have been studied, which include TS-based catalysts [12], Cu-based catalysts, and vanadia-based catalysts [13–17]. Pan et al. [18] prepared Cu-supported aluminum-pillared interlayer clay catalysts and used them for the direct hydroxylation of benzene to phenol with H_2O_2 as the oxidant. Their yield of phenol was 44% with a selectivity of 80%. Kong et al. [13] studied Cu–MCM-41 with a high copper content of up to 26.0%, which showed excellent catalytic activity in the direct hydroxylation of benzene with H_2O_2. These results showed that Cu is a highly active catalyst for benzene hydroxylation. Dimitrova et al. [19] investi-

* Corresponding author. Tel.: +86-452-2742573; E-mail: jlh29@163.com
# Corresponding author. Tel.: +86-452-2742563; E-mail: xfguo@163.com
This work was supported by the National Natural Science Foundation of China (21176125), the Science Research Project of the Ministry of Education of Heilongjiang Province of China (2012TD012, 12511Z030, 12521594), and the Graduate Innovation Fund of Heilongjiang Province of China (YJSCX2011-198HLJ).
DOI: 10.1016/S1872-2067(11)60487-7 | http://www.sciencedirect.com/science/journal/18722067 | Chin. J. Catal., Vol. 34, No. 2, February 2013

gated vanadium-grafted β and ZSM-5 zeolites as catalysts for the direct oxidation of benzene to phenol with H_2O_2 in acetonitrile. The catalytic activity of the former (phenol yield 24.5% and selectivity 70%) was better than that of the latter (phenol yield 11.3% and selectivity 75%), and the vanadium sites retained their multiple oxidation states when used in the liquid phase oxidation. Due to their high activity and remarkable stability, vanadia-based catalysts have been utilized as catalysts for a variety of oxidation reactions, especially for the hydroxylation of alkanes and aromatic compounds [7,20–21]. The supported V catalyst showed high catalytic activity when using H_2O_2 as oxidant. The anatase phase gave a better performance as a support of V_2O_5 for selective partial oxidation reactions compared to the rutile phase [22,23]. A large number of publications have shown that the V_2O_5 catalyst decreases the transformation temperature significantly [24], and the loaded VO_x results in a higher surface density of the nuclei for the phase transition from anatase to rutile. A good catalytic performance is obtained at vanadium loadings that give a vanadium monolayer on the TiO_2 surface [25]. In our laboratory, we have prepared VO_x-TiO_2 catalysts and used them for the hydroxylation of benzene to phenol with H_2O_2 as the oxidant in acetonitrile. The yield of phenol achieved was 23.8% with a selectivity of 85% under optimized conditions [26].

Although many single transition metal (Fe, Cu, V, etc.) catalysts have been used to catalyze the hydroxylation of benzene to phenol, no appreciable success has been achieved [27–29]. Studies on the structure of Cu/VO_x-TiO_2 and its catalytic properties have received little attention, especially as a catalyst for the direct hydroxylation of benzene to phenol. In this work, a series of Cu/VO_x-TiO_2 catalysts with different amounts of Cu oxide were synthesized using a hydrothermal synthesis method and used for the hydroxylation of benzene to phenol. Several factors were investigated in the preparation of the mesoporous Cu/VO_x-TiO_2 catalysts, such as Cu loading and calcination temperature, to get a catalyst with good catalytic activity and selectivity for the direct hydroxylation of benzene to phenol. The interaction of Cu and vanadium oxide with TiO_2 was investigated. The properties of the catalysts were studied using N_2 adsorption, scanning electron microscopy (SEM), transmission electron microscopy (TEM), X-ray diffraction (XRD), H_2 temperature-programmed reduction (H_2-TPR), and X-ray photoelectron spectroscopy (XPS).

2. Experimental

2.1. Catalyst preparation

The Cu/VO_x-TiO_2 catalysts were synthesized by hydrothermal synthesis using laurylamine (DDA, 98%, Sinopharm Chemical Reagent Co., Ltd., Shanghai, China) as the structural template, isopropyl alcohol (> 99%, Sinopharm Chemical Reagent Co., Ltd., Shanghai, China) as dispersing agent, and tetrabutyl titanate (TBOT, 98%, Sinopharm Chemical Reagent Co., Ltd., Shanghai, China), ammonium metavanadate (NH_4VO_3, ≥ 99.0%, Sinopharm Chemical Reagent Co., Ltd., Shanghai, China), and copper nitrate trihydrate ($Cu(NO_3)_2{\cdot}3H_2O$, ≥ 99.0%, Sinopharm Chemical Reagent Co., Ltd., Shanghai, China) as precursors. In a typical synthesis, a solution (A) containing 2.5 g of DDA, 21 g of absolute ethanol, 9.0 g of deionized water, 0.20 g of NH_4VO_3, and an amount of $Cu(NO_3)_2{\cdot}3H_2O$ were mixed thoroughly at 30 °C by vigorous stirring and then kept for 30 min. Another solution (B) was prepared by dissolving 17 g of TBOT in 6.0 g of isopropyl alcohol. Solution (B) was slowly added to solution (A) under vigorous stirring. A buff sediment was formed immediately. After stirring for 24 h, the mixture was aged without stirring at 30 °C for 24 h. The resulting mixture was filtered and the precipitate was washed with deionized water (200 ml). The precipitate was dried at 80 °C overnight and calcined at different temperatures (350–650 °C) at a heating rate of 2 °C/min for 6 h to remove organic species. The samples were denoted by Cu(x)/V(4.3)TiO_2-T, where x represents the weight percentage of Cu, x = 0.29%, 0.36%, 0.75%, 1.1%, 2.5% (measured by EDS), 4.3% (measured by EDS) is the weight percentage of vanadium, and T represents the calcination temperature, T = 350, 400, 450, 500, 550, 600, 650 °C.

2.2. Catalyst characterization

Powder XRD patterns were recorded on a Bruker D8 Advance (Germany) diffractometer using Cu K_α radiation (λ = 0.15418 nm). The N_2 adsorption isotherms were measured at –196 °C using a Quantachrome NOVA2000e instrument. The sample was degassed at 300 °C for 3 h under vacuum before the measurement. Sample morphologies were observed by SEM using a Rigaku S-4300 (Rigaku, Tokyo, Japan) spectrometer with an energy dispersive spectrometer. The microscopic features of the samples were observed by TEM using a Rigaku H-7650 electron microscope at 100 kV. H_2-TPR measurements were performed in a quartz tubular microreactor using a Quantachrome Chem-BET3000 instrument. H_2-consumption during reduction on heating was measured using a thermal conductivity detector. The surface chemical compositions of the catalysts were determined by XPS with a VG ESCALAB 250 spectrometer (Thermo Electron, UK) using a non-monochromatized Al K_α X-ray source (1486 eV).

2.3. Catalytic reactions

The liquid phase oxidation of benzene to phenol was carried out in a three-necked round bottomed flask (50 ml) with a magnetic stirrer. In a typical reaction, 0.18 g of catalyst, 5.0 ml of acetonitrile, and 2.3 g (0.03 mol) of benzene were added into the flask. After heating to 60 °C, 6.8 g of 30 wt% H_2O_2 (0.06 mol) were added to the reaction solution dropwise over 30 min. After 5 h, the reaction solution was cooled to ambient temperature and the solid catalyst was separated by centrifugation. The liquid product was analyzed by gas chromatography [Cotrun GC9800(N)]. Only benzoquinone was detected as a byproduct. Quantitative calculations were performed using methylbenzene added as an internal standard after the reaction.

3. Results and discussion

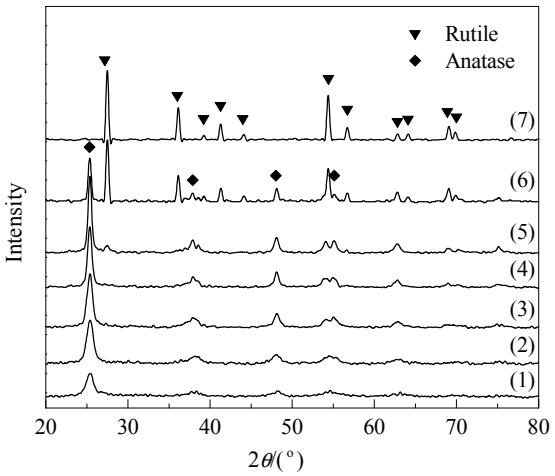

Fig. 1. XRD patterns of the Cu(0.75)/V(4.3)TiO_2-*T* catalyst samples calcined at different temperatures. (1) 350 °C; (2) 400 °C; (3) 450 °C; (4 500 °C; (5) 550 °C; (6) 600 °C; (7) 650 °C.

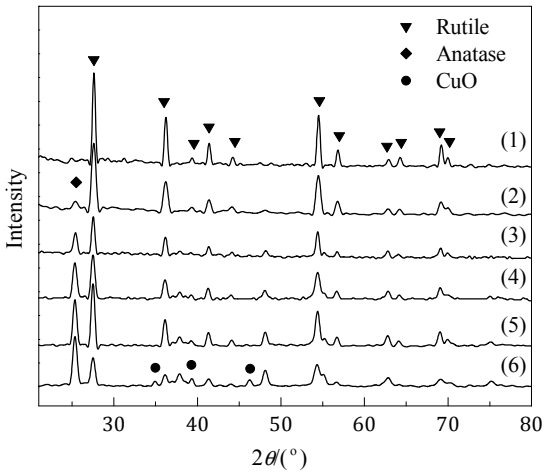

Fig. 2. XRD patterns of the Cu(*x*)/V(4.3)TiO_2-600 catalyst samples with different *x* values. (1) *x* = 0; (2) *x* = 0.29; (3) *x* = 0.36; (4) *x* = 0.75; (5) *x* = 1.1; (6) *x* = 2.5.

3.1. Characterization results of catalysts

The XRD patterns of the Cu(0.75)/V(4.3)TiO_2-*T* catalysts for different calcination temperatures are shown in Fig. 1. The main peaks at 2θ = 25.5°, 37.9°, 48.1°, 54.1°, and 62.6° were the (101), (004), (200), (105), and (204) diffraction peaks of anatase TiO_2 (JCPDS 21-1272) for calcination temperatures below 550 °C [30–32]. A considerable amount of anatase was transformed into rutile when the sample was calcined at 600 °C, and the anatase was transformed into rutile after calcining at 650 °C. Comparing the XRD patterns with those of the VO_x/TiO_2 samples showed that the Cu dopant hindered the phase transformation from anatase to rutile [22]. The XRD patterns for the catalysts with different Cu contents are shown in Fig. 2. Without Cu doping, the sample was mostly in the rutile phase. As the Cu loading increased, the crystalline phase changed significantly from the rutile to the anatase phase. This proved that the anatase-rutile phase transformation in the VO_x/TiO_2-supported catalysts was prevented by the added Cu. When the Cu loading was 2.5%, the anatase fraction was 75%, which indicated that the loading of the Cu species dramatically slowed down the transformation to rutile. The diffraction peaks at 2θ = 35.5°, 38.7°, and 46.3° corresponded to the formation of bulk CuO on the catalyst surface [33,34].

The N_2 adsorption isotherms of the Cu(0.75)/V(4.3)TiO_2-*T* samples are shown in Fig. 3(a). For calcination temperatures below 600 °C, the isotherms were classical Type IV, with a typical H_2 hysteresis loop, indicating the existence of pores with narrow entrances and large cavities [35,36]. When the calcination temperature was increased, the hysteresis loops of the samples were completely absent, which may be because of the crystallization of the sample, subsequent crystal growth, and collapse of the mesoporous structure [37]. The pore size distributions of the Cu(0.75)/V(4.3)TiO_2-*T* samples are shown in Fig. 3(b). For calcination temperatures below 600 °C, the samples had narrow pore size distributions (3–5 nm) and uniform pore structures. The pore size distributions became broader

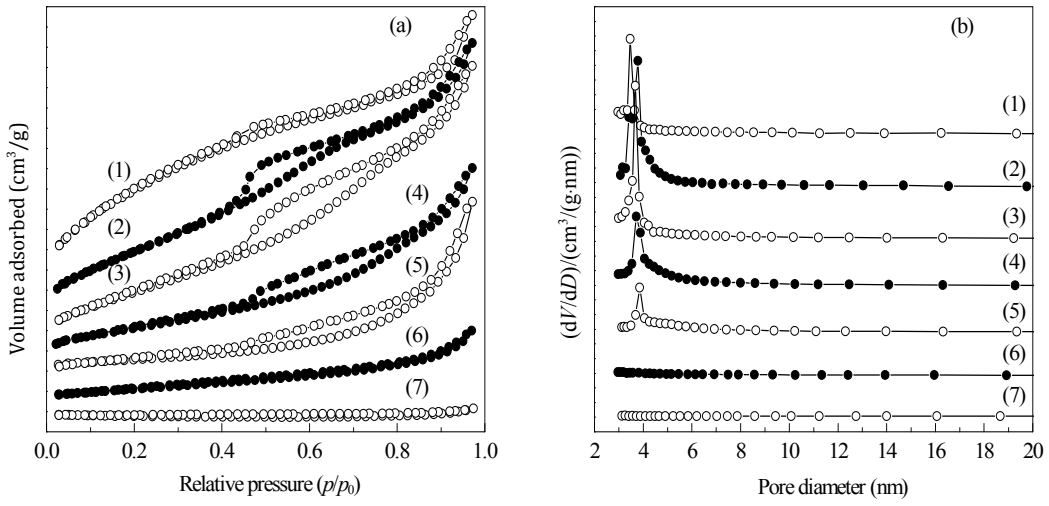

Fig. 3. N_2 adsorption-desorption isotherms (a) and pore size distributions (b) of the Cu(0.75)/V(4.3)TiO_2-*T* catalyst samples calcined at different temperatures. (1) 350 °C; (2) 400 °C; (3) 450 °C; (4) 500 °C; (5) 550 °C; (6) 600 °C; (7) 650 °C.

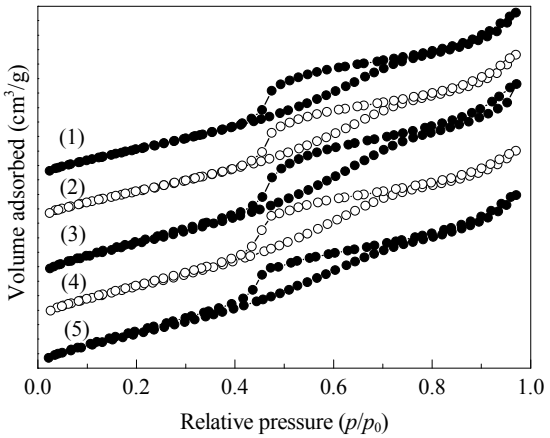

Fig. 4. N_2 adsorption-desorption isotherms of the Cu(x)/V(4.3)TiO_2-450 catalyst samples with different x values. (1) x = 0.29; (2) x = 0.36; (3) x = 0.75; (4) x = 1.1; (5) x = 2.5.

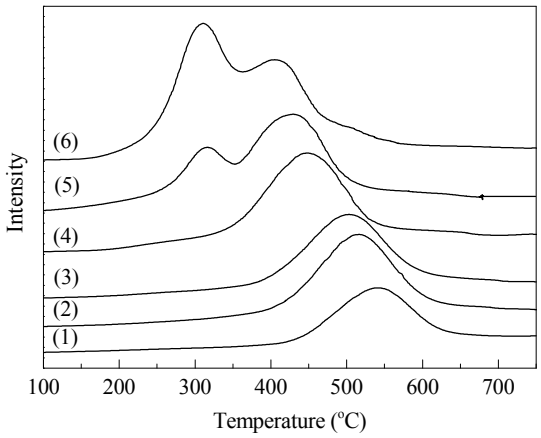

Fig. 6. H_2-TPR curves of the Cu(x)/V(4.3)TiO_2-450 catalyst samples. (1) x = 0; (2) x = 0.29; (3) x = 0.36; (4) x = 0.75; (5) x = 1.1; (6) x = 2.5.

with increasing calcination temperature, indicating that higher temperatures caused structural changes in the catalyst. For calcination temperatures of 600 °C and 650 °C, the pore size distributions of the samples were lost as a result of the collapse of the mesoporous structure and subsequent crystal growth. This was consistent with the XRD analysis. The Cu loading of the sample has some influence on the change in mesoporous structure of the catalysts, as shown in Fig. 4.

Figure 5 shows the SEM and TEM images of the Cu(0.75)/V(4.3)TiO_2-450 sample. The particles were spherical and the crystal sizes were about 14 nm, which was close to the XRD result (13.1 nm). The magnified TEM images (in Figs. 5(b) and 5(c)) showed that discernible pores were present on the surface of the sample when the particle size was around 14 nm, in agreement with the SEM results. The pore structure was investigated using high resolution TEM (Fig. 5(d)). Pores with an ordered wormhole-like mesoporous structure were seen on the sample surface. The d-spacings of the nanocrystals were 0.35 nm, which can be related to the (101) anatase plane [38,39].

The H_2-TPR profiles of Cu(x)/V(4.3)TiO_2-450 samples with different Cu loadings calcined at 450 °C are shown in Fig. 6. It can be seen that the reduction temperatures of the catalysts depended on the Cu loadings. The reduction peaks of the VO_x species [40] were shifted to lower temperatures for Cu loadings less than 0.75%, and the TPR curves exhibited only one major reduction peak. As the Cu loading was increased to 1.1%, other reduction peaks appeared at 300 °C. These may be attributed to the reduction of copper oxide species [34], and a reduction

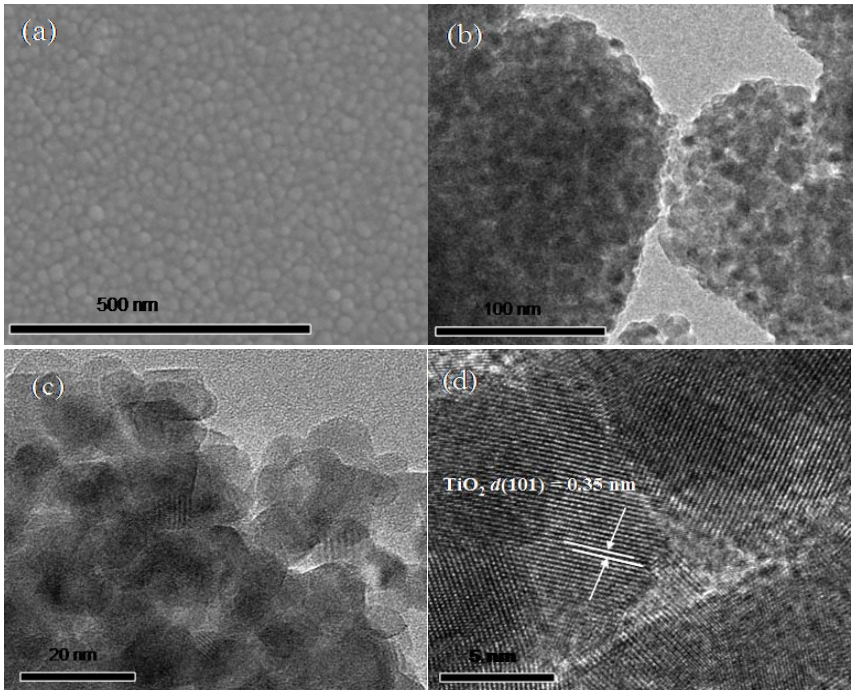

Fig. 5. SEM (a) and TEM (b, c, d) images of the Cu(0.75)/V(4.3)TiO_2-450 sample.

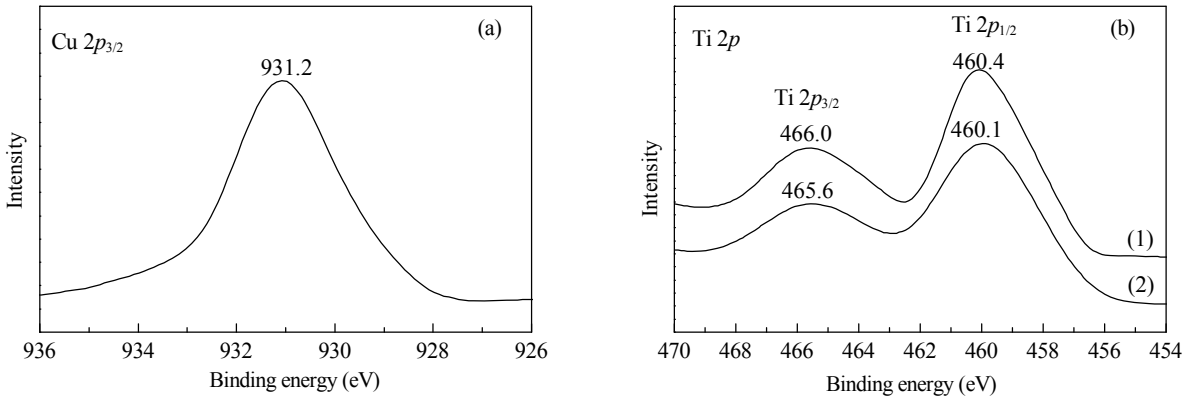

Fig. 7. XPS spectra of Cu 2*p* in Cu(0.75)/V(4.3)TiO_2-450 and Ti 2*p* in Cu(0.75)/V(4.3)TiO_2-450 (1) and Cu(0)/V(4.3)TiO_2-450 (2).

peak at 420 °C, corresponding to dispersed vanadium species located in the neighborhood of metallic Cu, which activated hydrogen. When the Cu loading reached 2.5%, the reduction peak at 300 °C became larger, which was attributed to reduction of large particles of crystalline CuO species. This indicated that the copper oxide species had aggregated and crystalline CuO was formed at high Cu loadings [41]. The peak at about 400 °C corresponded to dispersed vanadium species.

The Cu $2p_{3/2}$ XPS plot for the Cu(0.75)/V(4.3)TiO_2-450 catalyst is presented in Fig. 7. The Cu $2p_{3/2}$ peak indicated the formation of CuO (931.2 eV). A slight peak shift to a lower binding energy compared to the reference data was observed, which was related to the Cu $2p_{3/2}$ binding energy of CuO (933.4 eV) [30,42]. In Fig. 7(b), the two main peaks at 466.0 and 460.4 eV observed for the Ti 2*p* binding energy of the Cu(0.75)/V(4.3)TiO_2-450 sample were higher than those for the sample without Cu loading (465.6 and 460.1 eV) [30,43]. This is because the Fermi level of CuO is lower than that of TiO_2, so TiO_2 electrons are partially transferred to CuO, which results in changes in the outer electron cloud densities of the Ti and Cu ions. So the Ti 2*p* binding energies increased and the Cu binding energies decreased. This suggested that there was a strong interaction between the TiO_2 and Cu species [44]. The XPS spectrum of V $2p_{3/2}$ is shown in Fig. 8(a). The binding energies of 517.9 and 516.0 eV were attributed to V^{5+} and V^{4+} [45], respectively, in the Cu(0)/V(4.3)TiO_2-450 sample. For the Cu(0.75)/V(4.3)TiO_2-450 sample, the V $2p_{3/2}$ binding energies were increased to 519.3 and 518.1 eV [46]. This was because the electrons in VO_x were partially transferred CuO, so the V $2p_{3/2}$ binding energies increased.

3.2. Catalytic properties for the hydroxylation of benzene

The catalytic activities of the Cu(0.75)/V(4.3)TiO_2-*T* catalysts are shown in Fig. 9(a). The phenol yield and selectivity increased with increasing calcination temperature. The phenol yield was 25.6% at 450 °C. As the temperature was further increased, there was a notable decrease in phenol yield, which was because the samples were mainly in the rutile phase, with a significant decrease in the specific surface area, and the active VO_x components had formed a $V_xTi_{1-x}O_2$ rutile phase solid solution with TiO_2 [47,48], resulting in less active VO_x components. The relationship between the Cu content and the hydroxylation catalytic activity is shown in Fig. 9(b). The phenol yield and selectivity increased with increasing Cu content up to 0.75%. The maximum phenol yield was 25.6% and the yield decreased slightly with further increase in the Cu content of the catalyst. This was probably because the excess Cu species had aggregated and crystalline CuO was formed, which would accelerate the decomposition of H_2O_2 [14,18,28]. In addition, the aggregated Cu species have an unfavorable effect on the dispersion of the VO_x components, which would also be responsible for the decrease in the phenol yield and selectivity [22]. The influence of the amount of the Cu(0.75)/V(4.3)TiO_2- 450 catalyst on the

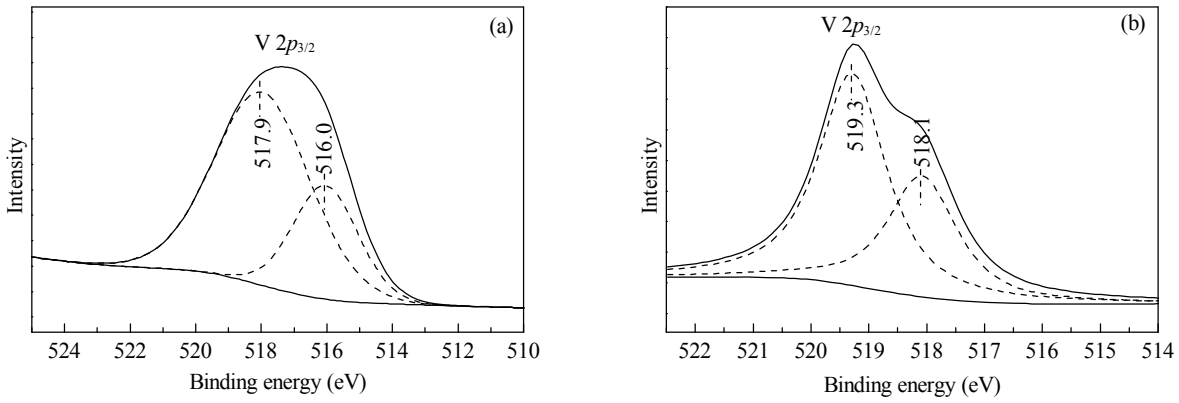

Fig. 8. XPS spectra of V 2*p* in Cu(0)/V(4.3)TiO_2-450 (a) and Cu(0.75)/V(4.3)TiO_2-450 (b) catalyst samples.

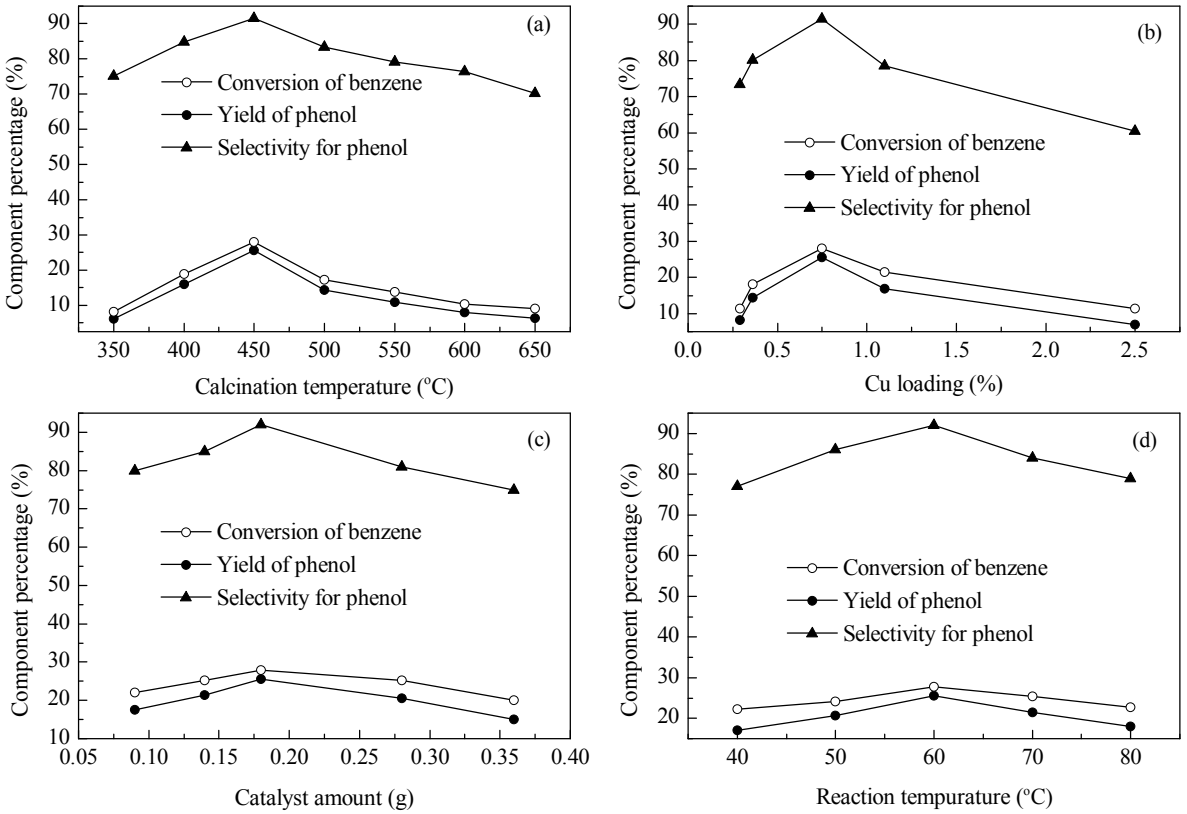

Fig. 9. Effects of Cu(0.75)/V(4.3)TiO_2-*T* samples (a), Cu(*x*)/V(4.3)TiO_2-450 samples (b), Cu(0.75)/V(4.3)TiO_2-450 amount (c), and reaction temperature (d) on the hydroxylation of benzene. Reaction conditions: benzene 0.03 mol, benzene:H_2O_2 = 1:2, acetonitrile 5 ml, *t* = 5 h.

phenol yield and selectivity is illustrated in Fig. 9(c). The yield of phenol increased with increasing catalyst amount. The maximum yield of phenol was 25.6%, with 0.18 g of catalyst. Further increasing the amount of catalyst decreased the phenol yield and selectivity. This can be attributed to the further oxidation of phenol by excess active species. The effect of varying the reaction temperature on benzene hydroxylation is shown in Fig. 9(d). The yield of phenol increased with increasing temperature up to 60 °C, but it decreased with further temperature increases. The maximum phenol yield was 25.6%. This may be the result of the thermal decomposition of H_2O_2 at higher temperatures. This behavior is similar to those of other Cu-based catalysts [18].

The structural characterization of the catalysts showed that the activity of the catalyst depended on the dispersion states of the vanadium and copper species and the crystal phase of the carrier. In the reaction using H_2O_2 as the oxidant, different peroxide intermediates can be formed with various metal oxides. The metal and H_2O_2 can form a metal-peroxo transition state after losing a water molecule, and then the metal-peroxo combine with benzene to complete the hydroxylation reaction [21,26,49,50]. After doping with the copper species, Cu^{2+} species exist as auxiliary species in the catalyst that promoted the catalytic activity of the Cu/VO_x-TiO_2 catalyst.

4. Conclusions

The liquid phase hydroxylation of benzene to phenol with H_2O_2 catalyzed by mesoporous Cu/VO_x-TiO_2 catalysts was investigated. The addition of a second metal, Cu, improved the thermostability of the Cu/VO_x-TiO_2 catalyst as compared with that of the VO_x-TiO_2 catalyst. The Cu also promoted the monodispersion of the vanadium species on the carrier surface and the facile reduction of VO_x at low temperatures. The vanadium species existed in the form of VO_x with two valences, +4 and +5. The copper species existed in the form of Cu^{2+}. The binding energies of the Ti and V ions were increased, which indicated there were interactions among the Cu species, V species, and TiO_2 that resulted in the increased binding energies of the Ti and V ions. When the copper species loading was 0.75%, the isolated VO_x and copper species were highly dispersed on the carrier surface. The Cu(0.75)/V(4.3)TiO_2-450 catalyst had high catalytic activity for the hydroxylation of benzene to phenol, and gave a phenol yield of 26% and phenol selectivity of 92%.

References

[1] Hoelderich W F. *Appl Catal A*, 2000, 194-195: 487
[2] Pirutko L V, Chernyavsky V S, Starokon E V, Ivanov A A, Kharitonov A S, Panov G I. *Appl Catal B*, 2009, 91: 174
[3] Liu Y Y, Murata K, Inaba M. *Catal Commun*, 2005, 6: 679
[4] Bortolotto L, Dittmeyer R. *Sep Purif Technol*, 2010, 73: 51
[5] Chen J Q, Gao Sh, Li J, Lü Y. *Chin J Catal* (陈佳琦, 高爽, 李军, 吕迎. 催化学报), 2011, 32: 1446
[6] Chen C H, Xu J Q, Jin M M, Li G Y, Hu C W. *Chin J Chem Phys*, 2011, 24: 358
[7] Zhu Y J, Dong Y J, Zhao L N, Yuan F L. *J Mol Catal A*, 2010, 315: 205

Graphical Abstract

Chin. J. Catal., 2013, 34: 341–350 doi: 10.1016/S1872-2067(11)60487-7

Cu-doped mesoporous VO_x-TiO_2 for catalytic hydroxylation of benzene to phenol

XU Dan, JIA Lihua*, GUO Xiangfeng*
Qiqihar University

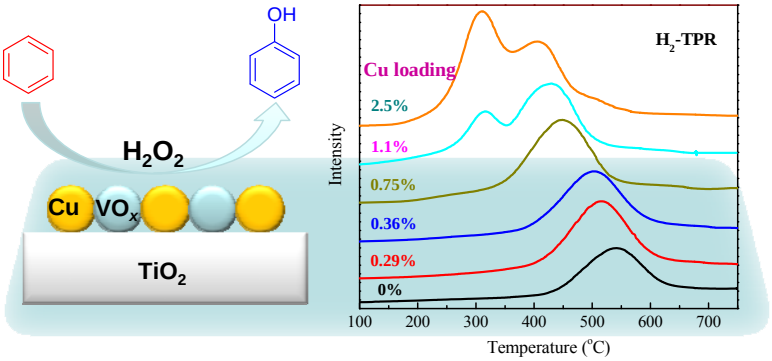

Incorporation of Cu additives into a VO_x/TiO_2 catalyst improved the reducibility of VO_x species, while Cu helped the monodispersion of VO_x species on the TiO_2 support surface.

[8] Feng S J, Pei S P, Yue B, Yue L, Qian L P, He H Y. *Catal Lett*, 2009, 131: 458
[9] Yamanaka H, Hamada R, Nibuta H, Nishiyama S, Tsuruya S. *J Mol Catal A*, 2002, 178: 89
[10] Garun T, Worapon K, Piyasan P, Hiroshi Y, Tomohiko T, Suttichai A. *Catal Commun*, 2008, 9: 1886
[11] Xu J Q, Liu H H, Yang R G, Li G Y, Hu Ch W. *Chin J Catal* (徐加泉, 刘慧慧, 杨瑞光, 李桂英, 胡常伟. 催化学报), 2012, 33: 1622
[12] Ratnasamy P, Srinivas D, Knözinger H. *Adv Catal*, 2004, 48: 1
[13] Kong Y, Xu X J, Wu Y, Zhang R, Wang J. *Chin J Catal* (孔岩, 徐鑫杰, 吴勇, 张瑞, 王军. 催化学报), 2008, 29: 385
[14] Qi X Y, Li J Y, Ji T H, Wang Y J, Feng L L, Zhu Y L, Fan X T, Zhang C. *Microporous Mesoporous Mater*, 2009, 122: 36
[15] Zhu Y J, Dong Y L, Zhao L N, Yuan F L, Fu H G. *Chin J Catal* (朱宇君, 董永利, 赵丽娜, 袁福龙, 付宏刚. 催化学报), 2008, 29: 1067
[16] Dittmeyer R, Bortolotto L. *Appl Catal A*, 2011, 391: 311
[17] Chen J Q, Gao S, Xu J. *Catal Commun*, 2008, 9: 728
[18] Pan J X, Wang C, Guo S P, Li J H, Yang Z Y. *Catal Commun*, 2008, 9: 176
[19] Dimitrova R, Spassova M. *Catal Commun*, 2007, 8: 693
[20] Sakamoto T, Takagaki T, Sakakura A, Obora Y, Sakaguchi S, Ishii Y. *J Mol Catal A*, 2008, 288: 19
[21] Jian M, Zhu L F, Wang J Y, Zhang J, Li G Y, Hu C W. *J Mol Catal A*, 2006, 253: 1
[22] Mastelaro M S P, Mastelaro V R. *Chem Mater*, 2002, 14: 2514
[23] Deo G, Turek A M, Wachs I E, Machej T, Haber J, Das N, Eckert H, Hirt A M. *Appl Catal A*, 1992, 91: 27
[24] Martin S T, Morrison C L, Hoffmann M R. *J Phys Chem*, 1994, 98: 13695
[25] Bulushev D A, Kiwi-Minsker L, Zaikovskii V I, Renken A. *J Catal*, 2000, 193: 145
[26] Xu D, Jia L H, Guo X F. *Catal Lett*, 2012, 142: 1251
[27] Renuka N K. *J Mol Catal A*, 2010, 316: 126
[28] Antonyraj C A, Kannan S. *Appl Clay Sci*, 2011, 53: 297
[29] Joseph J K, Singhal S, Jain S L, Sivakumaran R, Kumar B, Sain B. *Catal Today*, 2009, 141: 211
[30] Xin B F, Wang P, Ding D D, Liu J, Ren Z Y, Fu H G. *Appl Surf Sci*, 2008, 254: 2569
[31] Lv C X, Zhou Y, Li H, Dang M M, Guo C C, Ou Y C, Xiao B. *Appl Surf Sci*, 2011, 257: 5104
[32] Wu J C S. *Catal Surv Asia*, 2009, 13: 30
[33] Miyahara T, Kanzaki H, Hamada R, Kuroiwa S, Nishiyama S, Tsuruya S. *J Mol Catal A*, 2001, 176: 141
[34] Guerrero S, Guzmán I, Aguila G, Araya P. *Catal Commun*, 2009, 11: 38
[35] Yue W B, Xu X X, Irvine J T S, Attidekou P S, Liu C, He H H, Zhao D Y, Zhou W Z. *Chem Mater*, 2009, 21: 2540
[36] Kim D S, Han S J, Kwak S-Y. *J Colloid Interf Sci*, 2007, 316: 85
[37] Wang Y-D, Ma C-L, Sun X-D, Li H-D. *Appl Catal A*, 2003, 246: 161
[38] Qian X F, Wan Y, Wen Y L, Jia N Q, Li H X, Zhao D Y. *J Colloid Interf Sci*, 2008, 328: 367
[39] Zhu C L, Yu H L, Zhang Y, Wang T S, Ouyang Q Y, Qi L H, Chen Y J, Xue X Y. *ACS Appl Mater Interfaces*, 2012, 4: 665
[40] Bond G C. *Appl Catal A*, 1997, 157: 91
[41] Dong Y L, Niu X Y, Zhu Y J, Yuan Y L, Fu H G. *Catal Lett*, 2011, 141: 242
[42] Suh M-J, Ihm S-K. *Top Catal*, 2010, 53: 447
[43] Reddy B M, Kham A. *Catal Surv Asia*, 2005, 9: 155
[44] Srinivas B, Lalitha K, Reddy P A K, Rajesh G, Kumari V D, Subrahmanyam M, De B R. *Res Chem Intermed*, 2011, 37: 1069
[45] Silversmit G, Depla D, Poelman H, Marin G, Gryse R. *Surf Sci*, 2006, 600: 3512
[46] Cousin R, Abi-Aad E, Capelle S, Courcot D, Lamonier J-F, Aboukaıs A. *J Mater Sci*, 2007, 42: 6188
[47] Bulushev D A, Kiwi-Minsker L, Zaikovskii V I, Lapina O B, Ivanov A A, Reshetnikov S I, Penken A. *Appl Catal A*, 2000, 202: 243
[48] Bucharsky E C, Shell G, Oberacker R, Hoffmann M J. *J Eur Ceram Soc*, 2009, 29: 1955
[49] Tuel A, Tadrit Y B. *Appl Catal A*, 1993, 102: 201
[50] Zhang J, Tang Y, Li G Y, Hu C W. *Appl Catal A*, 2005, 278: 251

Cu掺杂对介孔VO_x-TiO_2催化苯羟基化制苯酚的影响

徐　丹[a], 贾丽华[a,*], 郭祥峰[b,#]

[a]齐齐哈尔大学化学与化学工程学院, 黑龙江齐齐哈尔 161006

[b]黑龙江省普通高校精细化工重点实验室, 黑龙江齐齐哈尔 161006

摘要: 将Cu作为第二金属, 制备了不同Cu掺杂量的和不同温度下焙烧的双金属改性的Cu/VO_x-TiO_2复合催化剂, 并用于液相苯直接羟基化制苯酚反应中. 固定钒的含量为4.3%, 合成了一系列不同Cu掺杂量 (w = 0.29%~2.5%) 的催化剂, 并在不同的温度下(350~650 °C)进行了焙烧. 利用X射线衍射、N_2吸附-脱附、扫描电镜、透射电镜、H_2程序升温还原以及X射线光电子能谱对催化剂进行了表征. 结果表明, 加入Cu后催化剂仍保持有序的介孔结构, 并且有效地促进了VO_x物种在载体TiO_2上的分散和VO_x物种的还原, 同时提高了催化剂的热稳定性, 其中Cu以+2价的形态存在于催化剂中. 另外, 考察了催化剂用量, 反应温度等对苯羟基化反应性能的影响.

关键词: 铜; 钒物种; 介孔二氧化钛; 苯; 羟基化; 苯酚

收稿日期: 2012-09-27. 接受日期: 2012-11-07. 出版日期: 2013-02-20.

*通讯联系人. 电话: (0452)2742573; 电子信箱: jlh29@163.com

#通讯联系人. 电话: (0452)2742563; 电子信箱: xfguo@163.com

基金来源: 国家自然科学基金(21176125); 黑龙江省教育厅科研项目(2012TD012,12511Z030, 12521594); 黑龙江省研究生创新项目(YJSCX2011-198HL).

本文的英文电子版由Elsevier出版社在ScienceDirect上出版(http://www.sciencedirect.com/science/journal/18722067)

1. 前言

苯酚是一种重要的有机化工原料, 目前世界上超过90%的苯酚是通过异丙苯法生产的. 该法工艺流程比较长, 同时产生等摩尔量的丙酮及其它副产物, 影响了其发展势头. 因此, 工艺简单、苯直接羟基化合成苯酚新工艺的开发广受关注[1]. 该路线绿色、原子经济性高, 包括N_2O氧化法[2]、O_2直接氧化法[3~6]、H_2O_2液相氧化法[7~9]等. 其中H_2O_2氧化苯一步合成苯酚唯一的副产物是水, 无环境污染, 被认为是未来最有希望工业化的新工艺[10,11]. 人们大都以H_2O_2为氧化剂, 在较温和条件下进行苯直接羟基化反应; 所采用的固体催化剂, 包括TS分子筛[12], 铜基和钒基催化剂[13~17]等. Pan等[18]将Cu负载到铝基柱撑粘土上, 以H_2O_2为氧化剂, 用于苯直接羟基化合成苯酚的反应, 苯酚的收率为40%, 选择性为80%. 孔岩等[13]合成出Cu-MCM-41催化剂, 当Cu负载量为26.0%时, 该催化剂在H_2O_2氧化苯直接羟基化反应中表现出较高的催化活性. Dimitrova等[19]将钒物种分别嫁接到β分子筛和ZSM-5分子筛上, 用于H_2O_2氧化苯直接羟基化反应, 其中V-β型分子筛表现了较好的催化性能, 苯酚收率和选择性分别为24.5%和70%; 而V-ZSM-5型分子筛催化剂上苯酚的收率为11.3%, 选择性为75%. 这两种催化剂中钒是以多重价态形式存在的. 含钒的混合氧化物材料具有较高的催化活性和稳定性, 因而广泛用于多种选择性氧化反应中, 尤其是烷烃类和芳香族化合物的羟基化反应中[7,20,21]. 以H_2O_2为氧化剂, 钒负载的催化剂对苯羟基化反应表现出较高的催化活性. 对于VO_x-TiO_2催化剂体系, 当载体TiO_2为锐钛矿相时, 其活性较高, 而为金红石相时, 则不利于反应的进行[22,23]. 研究表明, V_2O_5的加入可明显降低TiO_2的晶相转化温度[24]; 因为VO_x的负载能够增大TiO_2由锐钛矿相向金红石转化的核心的表面密度, 当钒物种单分散于载体TiO_2上时, 催化剂表现出较好的催化活性[25]. 本课题组已经成功制备了VO_x-TiO_2催化剂, 并用于液相苯直接羟基化制苯酚的反应, 以H_2O_2为氧化剂, 乙腈为溶剂, 最佳的反应条件下, 苯酚的收率和选择性分别为23.8%和85%[26].

用于苯直接羟基化反应有很多单负载过渡金属(Fe, Cu, V等)的催化剂, 但是催化效果均不太理想[27~29]. 据我们所知, 有关双金属负载的Cu/VO_x-TiO_2催化剂的报道较少, 尤其是用于苯直接羟基化制苯酚的反应中. 本文采用水热法制备一系列不同Cu含量的Cu/VO_x-TiO_2催化剂, 并用于苯直接羟基化的反应中. 考察Cu的负载量和焙烧温度对所制催化剂的影响, 以便合成出对苯羟基化反应具有活性较高的催化剂. 同时, 利用H_2程序升温还原(H_2-TPR)和X射线光电子能谱(XPS)技术, 研究Cu, V和载体之间的相互作用; 采用N_2吸附-脱附、X射线衍射(XRD)、扫描电镜(SEM)、透射电镜(TEM)、H_2-TPR和X射线光电子能谱(XPS)对合成的催化剂进行表征.

2. 实验部分

2.1. 催化剂的制备

以十二胺(DDA; 98%, 国药集团化学试剂有限公司)为模板剂, 异丙醇(99%, 国药集团化学试剂有限公司)为分散剂; 钛酸四丁酯(TBOT; 98%, 国药集团化学试剂有限公司)、NH_4VO_3(≥99.0%, 国药集团化学试剂有限公司)和 $Cu(NO_3)_2{\cdot}3H_2O$ (≥ 99.0%, 国药集团化学试剂有限公司)为前驱体,采用水热合成法制备了 Cu/VO_x-TiO_2 催化剂. 称取 2.5 g DDA, 0.20 g NH_4VO_3, 一定量的 $Cu(NO_3)_2{\cdot}3H_2O$, 21 g无水乙醇, 9 g 去离子水, 混合均匀配制成溶液 A. 将 17 g TBOT 溶于 6.0 g 异丙醇中, 充分混合均匀配制成溶液 B. 搅拌下, 将溶液 B 缓慢滴加到溶液 A 中, 立刻形成浅黄色沉淀. 30 °C 水浴中继续搅拌 24 h, 形成浅蓝色沉淀物, 陈化 24 h, 抽滤, 用 200 ml 去离子水进行洗涤, 于 80 °C 干燥过夜, 并在一定温度下焙烧 6 h (升温速率 2 °C/min), 所得 Cu/VO_x-TiO_2 催化剂标记为 Cu(x)/V(4.3)TiO_2-T 复合介孔材料, 并经 EDS 测定了 Cu 和 V 的含量. 其中 x 代表 Cu 的质量百分数, x= 0.29%, 0.36%, 0.75%, 1.1%, 2.5%, V 含量均为 4.3%, 焙烧温度 T= 350, 400, 450, 500, 550, 600, 650 °C.

2.2. 样品的表征

XRD 使用德国 Bruker D8 Advance 型粉末衍射仪测定, Cu K_α 辐射 (λ = 0.15418 nm). N_2 吸附-脱附曲线在 NOVA 2000e 型比表面积和孔隙度分析仪上测量, 吸附质为 N_2, 吸附温度为–196 °C; 测量前样品在 300 °C 真空脱气 3 h. SEM 照片在日本日立公司 S-4300 型场发射扫描电子显微镜上拍摄, 电压 20 kV, 样品室真空度优于 10^{-4} Pa. 在日本日立公司 H-7650 型 TEM 上拍摄样品形貌, 电压 100 kV. H_2-TPR 在美国康塔公司 Chem-BET3000 型化学吸附仪上测试, TCD 检测器, 桥电流 140 mA, 升温速率 10 °C/min. XPS 谱在美国热电公司的 VG ESCALAB 250 型分光仪上测试, 使用非单色 Al K_α X 射线源 (1486 eV).

2.3. 苯羟基化反应

向 50 ml 三口瓶中依次加入一定量的催化剂、5.0 ml 乙腈、2.3 g 苯 (0.03 mol), 在磁力搅拌下加热至一定温度, 然后逐滴加入 6.8 g 30% H_2O_2, 于 30 min 内滴加完毕. 继续反应 5 h 后, 混合液经离心分离, 取上层有机相在科创 GC9800(N) 型气相色谱仪上分析, 内标法 (甲苯作内标物) 对苯酚进行定量计算. 另外, 对产物进行检测发现, 除苯醌外无其他副产物生成.

3. 结果与讨论

3.1. 催化剂的表征结果

图 1 为各 Cu(0.75)/V(4.3)TiO_2-T 催化剂的 XRD 谱. 可以看出, 当焙烧温度低于 550 °C 时, 所得样品在 2θ = 25.5°, 37.9°, 48.1°, 54.1°和 62.6°处出现特征衍射峰, 分别对应于锐钛矿 TiO_2 (JCPDS 21-1272) 中 (101), (004), (200), (105) 和 (204) 晶面[30~32]. 焙烧温度升至 600 °C 时, TiO_2 部分晶相由锐钛矿相转化为金红石相; 至 650 °C 时, 催化剂的晶相全部转化为金红石相. 还可以看出, Cu 的掺杂抑制了催化剂由锐钛矿相向金红石相转化[22,26].

图 2 为不同 Cu 含量的 Cu(x)/V(4.3)TiO_2-600 催化剂的 XRD 谱. 由图可见, 没有负载 Cu 时, 600 °C 焙烧所制催化剂的晶相全部为金红石相; 随着 Cu 负载量的增加, 催化剂的晶相明显地由金红石相向锐钛矿相转化; 至 x= 2.5% 时, 所得样品中锐钛矿相的含量达到 75.4%, 说明 Cu 的掺杂有效地促进催化剂由金红石相向锐钛矿相转变. 另外, 该样品在 2θ = 35.5°, 38.7°和 46.3°处出现 CuO 晶面衍射峰, 说明其中有聚合态或晶态 CuO 生成[33,34].

图 3(a) 为 Cu(0.75)/V(4.3)TiO_2-T 催化剂的 N_2 吸附-脱附等温线. 由图可见, 当焙烧温度低于 600 °C 时, 样品的 N_2 吸附-脱附等温线为 IV 型, 并有 H_2 回滞环, 表明样品具有介孔结构[35,36]. 随着焙烧温度继续增加, 样品的滞后环完全消失了, 可能是由于高温焙烧使样品晶化度增加, 晶粒增长, 使介孔结构发生坍塌所致[37]. 图 3(b) 为上述催化剂的孔径分布图. 当焙烧温度低于 600 °C 时, 所得样品具有较窄的孔径分布 (3~5 nm), 说明样品具有规则的孔道结构. 可以看出, 随着焙烧温度的增加, 样品孔径分布发生了宽化; 至 600 和 650 °C 时, 样品的介孔完全消失, 可能是由于晶体的增长所致. 与 XRD 结果一致.

不同 Cu 含量的 Cu(x)/V(4.3)TiO_2-450 催化剂的 N_2 吸附-脱附等温线示于图 4. 可以看出, 改变 Cu 含量, 催化剂仍然保持有序的介孔结构.

图 5(a) 为 Cu(0.75)/V(4.3)TiO_2-450 催化剂的 SEM 照片. 可以看出, 样品呈球形小颗粒, 其粒径大约为 15nm 左右, 与 XRD 计算结果较为接近 (13.1nm). 图 5(b) 和 (c) 为样品的 TEM 照片. 可以看出, 样品确为球形小颗粒, 且存在规则的孔道结构. 由该样品的高分辨 TEM 照片 (见 5(d)) 可知, 催化剂表面存在规则有序的虫孔状结构, 晶面间距为 0.35nm, 其晶格条纹与锐钛矿相有序的 (101) 晶相位面相对应[38,39].

图 6 为 Cu(x)/V(4.3)TiO_2-450 催化剂的 H_2-TPR 谱. 可以看出, 未掺杂 Cu 时, 催化剂中钒物种的还原峰在 550 °C, 属于单分散 VO_x 的还原峰[40]. 随着 Cu 的加入, 且其负载量不超过 0.75% 时, 钒物种只有一个较大的还原

峰出现, 且逐渐向低位区偏移, 应为 VO_x 的还原; 当 Cu 掺杂量达到 1.1% 时, VO_x 还原峰出现在 420 °C, 还在 300 °C 出现一个小的还原峰, 可能是由于 Cu 物种的还原所致 [34]. 继续增加 Cu 负载量至 2.5% 时, Cu 物种还原峰面积增大, 说明随着 Cu 含量的增加, Cu 物种发生了聚合并形成晶相的 CuO[41]; VO_x 物种还原峰则出现在 400 °C.

图 7(a) 为 Cu(0.75)/V(4.3)TiO_2-450 催化剂中 Cu $2p_{3/2}$ 的 XPS 谱. 由图可见, Cu $2p_{3/2}$ 谱峰出现在 931.2 eV 处, 说明样品中 Cu 是以 Cu^{2+} 形式存在, 相对于标准 CuO 中 Cu^{2+} 的电子结合能为 933.4 eV 略有偏移 [30,42]. 图 7(b) 为不同催化剂中 Ti 2*p* 的 XPS 谱. 可以看出, 样品中掺杂 Cu 以后, Ti $2p_{1/2}$ 和 Ti $2p_{3/2}$ 的电子结合能分别从 465.6 和 460.1 eV 位移至 466.0 和 460.4 eV[30,43]. 这可能是因为 CuO 的费米能级低于 TiO_2, 导致 TiO_2 中的电子向 CuO 转移, 使 Ti 元素和 Cu 元素外部电子云密度发生变化, 所以 Ti 2*p* 的电子结合能增加而 Cu 2*p* 的电子结合能降低, 表明载体 TiO_2 和 Cu 之间存在很强的相互作用[44].

图 8 是 V $2p_{3/2}$ 的 XPS 谱, 并对 V $2p_{3/2}$ 的峰进行了分峰处理. 由图可见, 未掺杂 Cu 的 Cu(0)/V(4.3)TiO_2-450 样品的 V $2p_{3/2}$ 的电子结合能为 517.9 eV, 归属于 V^{5+}, 而位于 516.0 eV 的峰属于 V^{4+} [45], 说明催化剂中 VO_x 物种以 +4 和+5 形式存在. 在掺杂 Cu 的 Cu(0.75)/V(4.3)TiO_2-450 催化剂中, V $2p_{3/2}$ 的电子结合能增加为 519.3 和 518.1 eV[46], 可能是由于 VO_x 的电子向 CuO 转移所致.

3.2. 催化剂的活性

图 9(a) 为 Cu(0.75)/V(4.3)TiO_2-*T* 催化剂上苯羟基化反应结果. 由图可知, 随着催化剂焙烧温度的增加, 苯酚收率和选择性增加; 至 450 °C 时, 苯酚收率达到 25.6%; 继续增加焙烧温度, 苯酚的收率明显下降, 可能是因为高温焙烧致使催化剂的晶相由锐钛矿相转化为金红石相, 导致催化剂的比表面积下降, 或者因为高温焙烧使 VO_x 物种与载体 TiO_2 相结合形成了 $V_xTi_{1-x}O_2$ 固溶体结构[47,48], 使活性 VO_x 物种的量减少.

图 9(b) 为 Cu(*x*)/V(4.3)TiO_2-450 催化剂上苯羟基化反应结果. 由图可见, 随着 Cu 含量的增多, 所得催化剂上苯酚的收率有所增加; 至 0.75% 时, 苯酚的收率最佳, 达到 25.6%; 继续增加 Cu 的含量, 苯酚的收率明显下降, 可能是因为过多的 Cu 物种发生了聚合并形成 CuO, 从而可能加速了氧化剂 H_2O_2 的分解 [14,18,28]. 另外, Cu 物种的聚合不利于 VO_x 物种的分散, 也会导致苯酚收率和选择性下降[33].

图 9(c) 为 Cu(0.75)/V(4.3)TiO_2-450 催化剂用量对苯酚收率和选择性的影响. 由图可知, 随着催化剂用量的增加, 苯酚的收率逐渐增加; 至 0.18 g 时达最大, 为 25.6%; 继续增加催化剂的用量, 苯酚的收率和选择性下降, 可能是由于过多的活性物种使生成的苯酚发生了过氧化.

图 9(d) 为反应温度对 Cu(0.75)/V(4.3)TiO_2-450 上苯羟基化反应性能的影响. 可以看出, 随着反应温度升至 60 °C, 苯酚收率达到最大, 为 25.6%; 继续增加反应温度, 苯酚收率下降. 这可能是由于高温使得 H_2O_2 分解过快, 从而导致催化活性降低, 与文献报道的钒基和铜基催化剂催化苯羟基化反应结果相一致 [18,26].

结合催化剂表征结果可以看出, 催化剂活性主要取决于 V 物种和 Cu 物种的分散状态及载体 TiO_2 的晶相. 在苯羟基化反应中, H_2O_2 氧化剂与金属氧化物作用, 形成了不同的过氧物种, 金属物种与 H_2O_2 相结合形成金属过氧物种的过渡态, 失去一分子水后与苯环相结合, 再经过电子迁移形成中间体及过渡态, 进而完成苯羟基化反应[21,26,49,50]. 加入的 Cu^{2+} 作为助剂有利于 Cu/VO_x-TiO_2 催化剂活性的增加.

4. 结论

以 H_2O_2 为氧化剂, 以介孔 Cu/VO_x-TiO_2 为催化剂进行液相苯羟基化制苯酚反应. 结果表明, Cu 作为第二金属的加入增加了 Cu/VO_x-TiO_2 的热稳定性, 延缓了 TiO_2 锐钛矿相向金红石相的转化, 同时促进了 V 物种在载体 TiO_2 表面的分散和还原. 在催化剂中 VO_x 物种以混合的价态 (+4, +5) 存在, Cu 物种以 Cu^{2+} 形式存在, 它们与 TiO_2 之间存在很强的相互作用. 当 Cu 的含量为 0.75% 时, 孤立的 V 物种和 Cu 物种高度分散于载体 TiO_2 的表面, 催化剂活性较高, 苯酚收率和选择性分别达 25.6% 和 92%.